Engineered organic/inorganic hybrids for superhydrophobic coatings by wet and vapour procedures

UNIVERSITÀ DEGLI STUDI DI TORINO

Engineered organic/inorganic hybrids for superhydrophobic coatings by wet and vapour procedures

Guido Soliveri[a,b], Daniela Meroni[a,b*], Giuseppe Cappelletti[a,b], Rita Annunziata[a],Valentina Aina[c],Giuseppina Cerrato[c], Silvia Ardizzone[a,b]

[a] *Department of Chemistry, Università di Milano, Via Golgi 19, 20133 Milan, Italy, tel. +39/0250314225, fax: +39/0250314228, e-mail: daniela.meroni@unimi.it*

[b] *INSTM (Consorzio Interuniversitario Nazionale per la Scienza e Tecnologia dei Materiali), Via Giusti 9, 50121, Firenze, Italy*

[c] *Department of Chemistry IFM & NIS-Interdept. Excellence Centre, Università di Torino, via Pietro Giuria, 7, 10125 Turin, Italy*

** Corresponding author*

Abstract

Siloxane/oxide hybrids have attracted growing attention thanks to their ability to modulate the surface energy, wettability, or self-lubricity of a material. Here, we compare two functionalisation procedures (chemical vapour deposition and wet impregnation) on substrate films composed by preformed oxide particles. Three kinds of particles, characterized by different nature (SiO_2 and TiO_2) and average particle size, were studied to highlight possible effects related to the chemical and morphological state of the substrate surface. Morphological characterizations were carried out by dynamic light scattering (DLS) and scanning electron microscopy (SEM), while the structure of the hydrophobing layer was studied by combining Fourier Transform Infrared (FTIR) spectroscopy and solid state Nuclear Magnetic Resonance (NMR). The degree of functionalisation and the features of the siloxane layer vary significantly among the adopted oxides and functionalisation methods. The wettability features of the different hybrids closely mirror the results of the spectroscopic characterizations, giving rise to either Lotus leaf or patch-wise hydrophobic systems depending on the adopted conditions.

Keywords

wettability; silica; titania; siloxane; CVD; solid state NMR

Introduction

Hydrophobic and superhydrophobic materials have attracted considerable attention owing to both their fundamental interest and their plenty of technological applications [1]. Their application areas range from self-cleaning surfaces to anti-fouling coatings, from advanced patterning techniques to microfluidics diffusion.

In the case of surface functionalisation of inorganic materials by an organic molecule, the wetting features are the result of a complex balance among several aspects: the morphology of the substrate surface [2], the interactions between the surface and the organic moieties and the orientation/packing of the molecules in the hydrophobic layer [3, 4].

The morphology of the surface plays a crucial role as the presence of micro and nano-roughness may definitely change the wetting pattern, *e.g.* from hydrophobic to superhydrophobic [5].

Although the features of the substrate may affect the surface wettability, the procedure adopted to functionalise the layer may produce relevant modifications on the final performance of the material.

Functionalisation by alkoxysilanes is the most commonly used for oxide substrate and it is extensively described in the literature. The grafting of oxide surfaces by siloxanes is generally performed using two different experimental procedures. The most commonly employed method is a liquid phase procedure, which involves the immersion of the chosen substrate in a siloxane solution [6, 7]. As an alternative, vapour phase processes (chemical vapour deposition, CVD) have been more recently proposed. In this case, the substrate is functionalised by vaporizing the siloxane molecules in a close chamber under controlled temperature [8]. This procedure may represent a convenient alternative to the liquid phase method as it generally produces smooth and more stable siloxane layers [9]. In addition, vapour-phase reactions are generally less sensitive to variations in humidity and reagent purity than the solution-phase method, thus resulting in more reproducible hydrophobing layers [10].

Siloxane grafting on flat surfaces (*e.g.*, Si wafers) by CVD and wet techniques has been extensively studied [11, 12]. In the case instead of functionalized oxide micro/nanoparticles, the features of the hydrophobing layer have been by far less investigated, notwithstanding the enormous applicative interest of these materials.

In this paper, we present a comparison between vapour and liquid phase functionalisation procedures on substrate films composed by preformed oxide particles. Two different materials with very large applicative interest were chosen, SiO_2 [13] and TiO_2 [14, 15], in order to highlight possible effects related to the chemical state of the substrate surface. The differences between siloxane layers on silica and on titania particles are poorly investigated in the literature, as the TiO_2 systems have been by far less-extensively studied than SiO_2 supports, and existing studies are mostly limited to flat surfaces [16]. Moreover in this study, two different titania samples with largely different particle sizes and size distributions were adopted. The oxide surfaces were functionalised employing a commercial siloxane with broad industrial applications, by adopting either a CVD method or a wet procedure (WI). The obtained hybrids were characterized for their morphology (dynamic light scattering and scanning electron microscopy), their wettability (static and dynamic contact angle measurements) and for the features of the hydrophobing layer by using Fourier transform infrared spectroscopy and solid state Nuclear Magnetic Resonance (NMR).

Materials and Methods

All of the chemicals were of reagent grade purity and were used without further purification; doubly distilled water passed through a Milli-Q apparatus was employed.

Composite film deposition

The adopted hydrophobing agent (SILRES BS 1701) is produced and commercialized by Wacker Chemie AG. It is a mixture of isomeric octyltriethoxysilanes with isooctyltriethoxysilane as the main component.

Three different kinds of particles, characterized by different composition and surface area, were employed.

The samples are named according to the following notation: a letter identifying the nature of the oxide (S for silica, T for titania) and a number specifying the sample specific surface area. The adopted SiO_2 sample (named S-6) was a silica powder from Sigma Aldrich. Two different TiO_2 samples were employed: one commercial (T-3), purchased from Sigma Aldrich, and one laboratory-made (T-216), prepared by a sol-gel synthesis using the following procedure. A solution of $Ti(OC_3H_7)_4$ in 2-propanol was hydrolyzed at 65 °C by addition of water, adopting a water/alkoxide molar ratio of 100 and a water/2-propanol molar ratio of 20. The obtained slurry was dried overnight at 90 °C, then thermally treated at 300 °C for 5 h under O_2 stream.

Two different methods of surface functionalisation were adopted: wet impregnation and chemical vapour deposition.

In the wet procedure, oxides were functionalised with siloxane molecules as follows: 0.2 g of the oxide powder was dispersed in 10 mL of 2-propanol by sonication. The chosen amount of siloxane (33% w/w) was subsequently added to the titania slurry under vigorous stirring. The solvent was evaporated under reduced pressure (400 mbar, 40 °C) using a vacuum oven. Thin films were obtained by spin coating as previously reported [4].

Chemical vapour deposition, adapted from Sujimura et al. [8], was performed on spin-coated films of pristine oxide particles. The bare oxide particles were previously spin coated on the glass to make a film using the same deposition parameters described in wet procedure. Then, the oxide films were placed in a glass container together with a Teflon cup filled with siloxane. The container was placed in an oven at 100 °C for 3 hours to obtain the vaporization of the siloxane.

Sample characterization

The specific surface area of the oxide samples was determined by the BET (Brunauer-Emmett-Teller) procedure using a Coulter SA 3100 apparatus.

Phase composition was determined by room-temperature X-Ray Powder Diffraction (XRPD). Rietveld refinement was performed using the GSAS software suite and its graphical interface EXPGUI [17].

The particle size distribution of the oxide powders suspended in water was determined by Dynamic Light Scattering (DLS) by using a Nanosizer N4 (Beckman Coulter) and a Zetasizer Nano S ZEN1600 (Malvern Instruments), equipped with mobile lens and laser beam with wavelength 623.8 nm.

Scanning electron microscopy (SEM) images of the different oxide particles were acquired by a Zeiss LEO 1430 (30 keV), equipped with a backscattered electron detector as well as an energy dispersive X-ray analysis system. The size of the aggregates was evaluated by SEM image analysis using the ImageJ software (U.S. National Institute of Health, Bethesda, Maryland, USA, 1997-2012).

Static and dynamic contact angle (advancing θ_a and receding θ_r) measurements of hybrid siloxane-oxide films were performed on a Krüss EasyDrop instrument using several high purity solvents (water, toluene, glycerol, ethylene glycol, diiodomethane), according to a procedure reported previously [18].

Fourier Transformed Infrared (FTIR) spectra (128 scans, 4 cm^{-1} resolution) were collected on a Bruker IFS 113v spectrometer, equipped with MCT detector. Samples were pressed into self-supporting pellets (approximately 10 mg cm^{-2}) and placed in a quartz cell fitted with KBr windows. Prior to any FTIR measurements, all samples were activated in vacuo at room temperature (namely, IR beam temperature, some 30 °C higher than room temperature) to remove the weakly physisorbed surface species, by connecting the quartz cell to a conventional high vacuum glass line capable of a residual pressure $<10^{-4}$ Torr (1 Torr = 133.32 Pascal).

The siloxane chemisorption to the oxide surface was studied by solid state Magic Angle Spinning (MAS) NMR spectroscopy. ^{13}C and ^{29}Si solid state spectra were recorded at 125.62 and at 99.36 MHz, respectively, using a Bruker Avance 500 spectrometer equipped with a 4 mm magic angle spinning (MAS) broadband probe (spinning rate up to 4 kHz). The MAS spectra were obtained using approximately 0.15 g of solid sample, packed into a 4-mm MAS rotor (50 μL sample volume) spinning at 10 kHz and at 300 K. No resolution improvement was found at higher spinning rate and/or temperature. ^{13}C and ^{29}Si nuclei were observed using direct polarization (DP) or cross polarization (CP) methods, under the conditions described in our previously published studies [4,

19, 20]. ^{29}Si DPMAS measurements were performed using 350 scans and a pulse delay of 300 s. The variable amplitude CPMAS experiment was used to enhance the polarization of observed nuclei and increase the repetition rate of data acquisition. The maximum of ^{1}H → ^{29}Si polarization transfer was achieved using a contact time of 3 ms, in agreement with previous studies performed for similar materials [21]. For ^{13}C nuclei, shorter contact times of 1.0-1.5 ms were used. The values of ^{1}H longitudinal relaxation time encountered in all compounds did not exceed 1.5 s, which allowed for repetition time 2.0 s to be used in CPMAS experiments. Typically 4 K and 6 K scans each spectrum were accumulated for ^{1}H → ^{29}Si and ^{1}H → ^{13}C respectively. All chemical shifts were externally referenced to TMS.

Results and discussion

Oxide particle morphology

The three selected samples show different morphological features. S-6 sample is a silica powder characterized by a specific surface area of ~6 $m^2 g^{-1}$. The silica powder is compared with two different TiO_2 samples, a commercial and a laboratory-made one. The commercial sample T-3 is composed by rutile, a phase composition suggesting a high temperature preparation procedure, and, consequently, presents a very low surface area (~3 $m^2 g^{-1}$). The laboratory-made sample (T-216) is instead composed by 60% anatase and 40% brookite, two polymorphs usually obtained by calcination at mild temperatures, thus exhibiting a high specific surface area (~216 $m^2 g^{-1}$).

The particle size distribution of the selected oxides was analyzed by DLS. Figure 1 shows that all oxides are polydispersed, presenting at least two distinct size populations. S-6 and T-3 are largely micrometric, although they exhibit a small but significant fraction of nanometric aggregates. The laboratory-made sample T-216 is the most polydispersed, showing three distinct populations in both nanometre and micrometre range.

The particle morphology was determined by SEM analysis (Figure 2). For all samples, SEM images show inhomogeneous distribution with different degrees of aggregation between the primary particles. The size of the aggregates observed in SEM images well correlates with the particle size determined in suspension by DLS (Figure 1, column 4). However, larger agglomerates (in the micrometre scale) are formed by all samples during the particle deposition, probably triggered by the solvent evaporation. Further, the particle size distributions obtained by SEM images have a limited statistical significance given the very low number of particles that can be measured in each image.

The laboratory-made oxide T-216 (Figure 2c) exhibits a much lower tendency to form large agglomerates during solvent evaporation, resulting in a much smaller particle size range.

FTIR spectroscopy

FTIR spectroscopy was resorted to in order to study the functionalisation of the oxide surface by the addition of siloxane molecules.

Figure 3 reports the FTIR spectra of the two most representative samples (S-6 in Section A and T-216 in Section B) before and after the functionalisation with the hydrophobing agent. In the case of sample T-3, the amount of grafted siloxane is very low so that the relative bonds are scarcely appreciable.

Concerning the two pristine samples (see spectra a, dashed lines, in both sections), the following features can be appreciated in the 3900-1350 cm^{-1} range:

1. The OH stretching vibration of free surface hydroxyl groups, located at ~3700 cm^{-1} and ~3690 cm^{-1} for S-6 and T-216 samples, respectively [22, 23].

2. A broad band in the 3700-3000 cm^{-1} spectral range originating from the OH stretching vibration of hydroxyl groups interacting by hydrogen bonding.

3. The spectral component located at ~1630 cm^{-1} is due to the in-plane HOH bending mode of undissociated water molecule present at the sample surface.

4. Only in the case of the S-6 sample, there are three additional bands in the 2100-1700 cm^{-1} region that, on the grounds of the literature [22, 24] and of the spectral behaviour, can be attributed to Si-O-Si combination (overtones) modes, typical of the silica matrix.

After the functionalisation with both procedures (WI, lines b, and CVD, line c), some important spectroscopic changes are evident for both samples:

1. Sharp bands appear in the 2900-2700 cm^{-1} region, which can be assigned to ν_{C-H} stretching modes on the basis of the spectral position and literature data [24].

2. At lower frequencies (1700-1350 cm^{-1} spectral range), the bands of the bending δ_{C-H} counterparts of the above-described stretching modes of all CH-containing species are evident.

The above-described spectral changes that occur after the functionalisation for both samples, are better visible in the (b – a) and (c – a) traces (see insets of Figure 3), which represent the difference obtained by subtracting the background spectrum of pristine oxide (S-6 or T-216) from that of the functionalised samples (with both procedures, *i.e.*, WI and CVD methods), respectively.

By the detailed inspection of these differential spectra, it is worth noting the following:

1. A negative peak appears, located at ~3700 cm^{-1} (sharp) and ~3690 cm^{-1} (broad) for S-6 and T-216 functionalised samples, respectively. Negative peaks are indicative of species (or groups of species) that have been consumed upon functionalisation. This experimental evidence confirms that the hydrophobing agent is present on the surface of the examined samples and interacts with it through the OH species. The shape of this negative peak is related to the type(s) of OH groups present on either silica or titania matrices: on the basis of both their spectral behaviour and literature data [22, 24], these components are ascribable to free OH groups coordinated to surface Me^{n+} (*i.e.*, Si^{4+} or Ti^{4+}) cations. In particular, in the case of the S-6 samples, these OH species are coordinated to only one silicon ion, thus representing a terminal position, whereas in the case of the T-216 materials, the

broadness of the envelope indicates that different contributions may be present, *i.e.*, OH groups can be coordinated either to one titanium ion or bridged to two of them.

2. Also positive peaks appear: these are due to the species which form on the surface after the functionalisation procedures. They can be represented by both OH groups interacting by hydrogen bonding, in the 3700-3000 cm^{-1} spectral range, and C-H groups, whose modes lie in the 2900-2700 and 1700-1350 cm^{-1} regions. As for the former envelope, its relative intensity, if compared to that exhibited by the ν_{CH} modes, is much higher in the case of the T-216 samples rather than in the case of the S-6 ones (see the insets of Figure 3).

Thus, FTIR spectra confirm the successful functionalisation of both samples with both procedures (WI and CVD).

In the case of sample T-3, differential spectra show that the grafting process may occur by the same mechanism as for T-216. The much lower intensity of the siloxane related bands, in particular of the ν_{C-H}, may be traced back to the much lower surface area, the presence of the rutile polymorph and the scarce surface hydroxylation. The same effect is observed by NMR (see subsection 3.3).

The semi-quantitative differences observed in the ν_{C-H} and δ_{C-H} bands (namely, differences in the intensity of the peaks) obtained with the two functionalisation procedures represent an indication of a different structure of the adsorbed layer. In particular, as for what concerns the SiO_2 systems, films obtained by the CVD procedure exhibit a more ordered character than those obtained by the WI approach: this can be inferred by the detailed inspection of the ν_{CH} stretching region around 2910-2930 cm^{-1} (see the inset in Figure 3A). In fact, in the case of the CVD films a specific ν_{CH} component located at ~ 2920 cm^{-1} is more evident than in the case of the WI sample. On the basis of the spectral behaviour of this species and of literature data for similar systems [25], this component is ascribable to the formation of ordered aggregates of grafted molecules. On the other hand, in the case of the TiO_2 systems, the situation is less clear, since the spectral patterns in the ν_{CH} stretching region are more complicated, preventing us from

drawing reliable assignments. These differences will be confirmed and better explained by the solid state NMR spectroscopy study, as reported in the following.

Solid state NMR

Solid state NMR has emerged as an important tool to study organic molecules chemisorbed on oxides surfaces and to obtain structural information concerning hybrid materials. This technique provides spectroscopic evidence for the presence of organic moieties in the materials, confirms their chemical structure and investigates the characteristics of the attachment bonds [4, 19, 26, 27].

It is well-known that siloxane derivatives bind to oxide surfaces, such as TiO_2 and SiO_2, via Si/Ti-O-Si bonds resulting from the condensation between Si-OR and surface -OH groups and from the coordination of the silyl oxygen to a surface Ti/Si atom; this leads to a variety of mono-, bi-, and tridentate binding modes (see below). The present spectroscopic study, performed by ^{13}C and ^{29}Si solid state MAS NMR, investigates the attachment modes of the siloxane to the oxide surface and demonstrates that the oxide materials were well functionalised.

The ^{13}C spectra of all compounds (reported in Figure 4) show resonances in agreement with those observed in homogeneous solution of the corresponding precursor and are easily assigned (see Online Resources). All ^{13}C spectra provide clear evidence that the materials have been functionalised as expected. The marked differences among the spectra will be commented below.

The ^{29}Si resonances were attributed on the grounds of the literature [4, 28, 29]. The Figure 5 reports the ^{29}Si MAS NMR spectra of the siloxane-oxide hybrids. The absence, in the ^{29}Si spectra, of the signal relative to the siloxane starting compound (≈ -28 ppm), confirms the successful functionalisation of all materials and the absence of unbound siloxane molecules.

Also in this case, as by FTIR analyses, the two titania samples show completely different behaviour. The ^{29}Si signals of T-3 samples are not sufficiently intense even to be appreciable and are therefore, not further discussed.

The ^{29}Si spectra concerning the SiO_2 samples (Figure 5a,b) show two well differentiated set of signals. The ^{29}Si high-field resonances, observed around -85 and -110 ppm, are at positions typical of silicon groups Q^4 [siloxane, $(\equiv SiO)_4\underline{\mathbf{Si}}$)], Q^3 [single silanol, $(\equiv SiO)_3\underline{\mathbf{Si}}OH$)] and Q^2 [geminal silanol, $(\equiv SiO)_2\ \underline{\mathbf{Si}}(OH)_2$] relative to the starting silica material un-substituted, as reported in the literature [21, 30]. The low-field resonances (around -50 and -70 ppm) represent silicon atoms in position $(\equiv SiO)_2\ \underline{\mathbf{Si}}(OH)R$ and $(\equiv SiO)_3\ \underline{\mathbf{Si}}R$ which are denoted T^{2*} and T^{3*} respectively, in other words they can be related to the surface silicon atoms bounded to the siloxane molecules. Therefore the T^{2*} and T^{3*} resonances confirm the existence of a covalent linkage between the organic group and the silica surface. The ratio between the areas of the two resonance sets largely differs, depending on the functionalisation method, showing that the material obtained following the CVD procedure was far more functionalised than the WI one.

Also the ^{13}C MAS NMR spectra of these SiO_2 compounds, functionalised by the two methods, show marked differences (Figure 4). While the spectrum of the WI sample reveals only two unresolved and very broad signals (width at half height $\Delta\nu_{½} \approx 20$ ppm), the CVD sample shows well defined and sharp peaks (Figure 4b), which are indicative of a more ordered layer. In an ordered layer in fact, chains tend to align and pack together as a result of Van der Waals forces, causing a lack of mobility and for the steric hindrance a minor number of possible conformations, decreasing the line width. The ^{13}C NMR spectrum reported Figure 4b allows us to appreciate the well resolved resonances of the ethoxy group, methyl (58 ppm) and methylene (17 ppm) carbons, which are instead overlapped to the alkyl chain carbons in all others samples. The low intensity of the ethoxy group signals supports, in the case of SiO_2 functionalised by CVD, the high substitution degree of the ethoxy group during the functionalisation process.

Concerning TiO_2 samples, we observed in the ^{29}Si spectra a single signal in the range -50/-60 ppm (Figure 5c-d), corresponding to silicon atoms involved in Si-O-Si and Si-O-Ti bonds between the

siloxane molecules and the TiO_2 surface. This signal shows three resolved resonances, suggesting the co-presence of silicon species with different chemical structures. The relative percentages of the coexisting structures of silicon sites were obtained by deconvolution of DPMAS spectra. The fitting analysis, performed with Gaussian curves, and the structures related to the different components are reported in Figure 1 Online Resources.

From literature data previously reported for silicon atom coordination [4, 19, 31], the three different resonances at -51.0, -59.0 and -68 ppm, can be attributed to different structures depending on the attachment modes of the siloxane molecule to the TiO_2 surface, respectively named T^1, T^2 and T^3. In the T^1 structure, the siloxane moieties are bound to the oxide surface only by one Si-O-Ti bond. While in the T^2 the Si atom has two Si-O-Si/Si-O-Ti bonds and one residual OH/OR group. In this case there are two possible different structures, not discriminated by ^{29}Si NMR: they result from either siloxanes making two Ti-O-Si bonds with the TiO_2 surface (T^2_{Ti}) or siloxanes making one Ti-O-Si bond with the TiO_2 and one Si-O-Si bond with a neighbouring siloxane group (T^2_{Si}). In the T^3 structure the siloxanes form one Si-O-Ti bond with the titania surface and two Si-O-Si bonds with adjacent siloxane moieties.

Table 1 reports the amounts of the different T^X structures and the width at half height ($\Delta\nu_{1/2}$) of each resonance obtained by the fitting analysis of the ^{29}Si NMR spectra of siloxane-TiO_2 samples. It appears that the T^2 component is prevalent in the case of the sample from WI, in agreement with previous results [4]. On the other hand, the T^1 structure is prevalent in the CVD sample. This difference in behaviour can be ascribed to different mechanisms working in the formation of the siloxane layer, during CVD and WI procedures. It is in fact often reported that in liquid phase methods, siloxane tends to condense into flat aggregates in solution which subsequently adsorb onto the substrate [11]. The absence of this pre-polymerization step in vapour phase techniques (siloxane olygomers have lower surface tension than monomers) is in agreement with studies reporting that polymerization of silane molecules could be reduced in layers deposited by the vapour phase methods [32, 33].

Wetting properties

Film roughness dramatically alters the wetting features of a surface. Depending on the roughness degree of a surface, a Wenzel [34] or Cassie-Baxter [35] state can be obtained, resulting in completely different observed CAs (Figure 6a,b). In a film composed of particles, the resulting surface roughness can be expected to be linked to the size and morphology of the employed particles and to their degree of agglomeration. A textured topography showing a multi-scale (micro and nanometric) roughness, similar to that of lotus leaves, has proven to be necessary to impart stable superhydrophobic properties [36].

Before functionalisation, bare oxide films showed hydrophilic to superhydrophilic properties (~ 0°). Instead, all functionalised films exhibit a hydrophobic behaviour, although largely different wetting properties are appreciable among the different oxides and functionalisation methods.

Comparing the effect of the oxide type (Table 2), T-216 is the only oxide that gives superhydrophobic coatings upon functionalisation by both methods. In fact, T-216 films exhibit low CA hysteresis $\Delta\theta$ and water CAs much higher than 150°. NMR spectra of the T-216 samples functionalised by CVD and WI were indeed remarkably similar, showing only a minor difference in the relative percentages of the T^1 and T^2 structures. These evidences are to be related to the texture/morphology of the pristine particle composing the layer. In the case of T-216, the specific surface area of the pristine particles is very large and the size distribution of the particles broad. On the contrary, the other TiO_2 powder, T-3, is the only one among the studied oxides that never gives rise to superhydrophobic coatings. T-3 samples, produced by both functionalisation methods, exhibit a Wenzel-type wetting behaviour, characterized by large CA hysteresis and moderate water CA values (<< 150°). The low intensity of siloxane peaks observed in both FTIR and NMR spectra, show that the degree of functionalisation for T-3 is very low by both adopted procedures. Although S-6 sample has a similar surface area to T-3, it shows much better performances, showing a behaviour close to superhydrophobicity when functionalised by CVD method. Indeed, the relative intensity exhibited by the ν_{CH} modes and by OH groups interacting by hydrogen bonding suggests a larger functionalisation of the SiO_2 system with respect to TiO_2, especially in the case of the CVD samples. S-6

shows the largest gap in the CA values between CVD and WI methods (Figure 6c,d) in agreement with the relevant differences observed in ^{29}Si and ^{13}C solid state NMR spectra (Figures 4, 5). The measured CAs performed with different solvents (Table 1 Online Resources) show a trend similar to the discussed water CAs.

Comparing the two functionalisation methods, it can be appreciated that CVD is the most efficient in imparting hydrophobicity as it results in water CAs 20-30° higher than those of WI samples. This phenomenon could possibly be explained on the grounds of NMR and FTIR data. In the case of SiO_2, a higher degree of functionalisation was determined for the CVD sample on the grounds of ^{29}Si NMR, accompanied by well defined and sharp ^{13}C NMR peaks.

Conclusions

The role played by the adopted functionalisation procedure of different oxides by siloxane was investigated in detail. Both a wet impregnation and a chemical vapour deposition method were employed to highlight possible effects on the features of the resulting organic/inorganic hybrids. By solid state NMR and FTIR, the occurrence of chemisorption bonds between the organic moieties and the inorganic substrate were observed in any condition. The effects of both particle morphology and features of the siloxane layer on the wetting behaviour of the hybrid materials were studied.

By comparing the spectroscopic analyses, silica (S-6) sample presents much larger functionalisation degree than the titania sample with comparable specific surface area (T-3), resulting in a more hydrophobic wetting behaviour by both procedures. It has been reported that higher ionic character of the Ti-O bond with respect to Si-O, ascribable to the different electronegativity of the two atoms, may affect the interaction with an adsorbate [16]. The observed lower density of adsorption of a siloxane-mediated protein onto TiO_2 with respect to SiO_2 was attributed by Kim et al to this difference in ionic character [37].

Among the three different oxides, only the laboratory-made titania with a highly polydisperse character in the nanometric/micrometric range gave rise to a Lotus leaf effect, apart from the functionalisation technique utilized. The resulting hierarchical topography of the substrate surface is thought to be beneficial for the obtainment of a stable super-hydrophobic behaviour [36]. Different results were instead achieved for micrometric titania and silica, which presented critical differences by changing the functionalisation technique.

The dissimilarity between the two techniques has been well investigated by means of ^{29}Si and ^{13}C solid state NMR and FTIR analyses. The use of CVD results in higher hydrophobicity for all the samples analysed, deriving from a larger functionalisation. Furthermore, the observed variation in the relative weight of the siloxane attachment modes, resulting from the fitting of ^{29}Si CPMAS NMR spectra, suggests the occurrence of a different functionalisation mechanism in the two cases. The lower degree of cross-linking observed in the case of CVD on T-216 (prevailing T^1 component in NMR spectra) can be traced back to the absence of a pre-polymerization step in solution. This latter step is critically affected by the water content of the solvent. Thus, CVD is inherently less dependent on parameters such as the quality of the silane and the solvent-siloxane interactions.

The vapour deposition, although less investigated in literature, seems to create better functionalised films, and could be identified as a possible replacement to the classical reaction in high anhydrous and apolar conditions. This could be a great advantage in some applications, that need a good quality of the hydrophobing layer without the use of environmentally unfriendly solvents.

Acknowledgements

This research has been supported by the University of Milan Research Funds (PUR).

Online Resources. Assignments of ^{13}C NMR resonanes; Fitting analysis of the ^{29}Si NMR spectra of siloxane-TiO_2 composites obtained by WI and CVD, and sketches of the structures attributed to the different resonances; Static contact angles for different solvents on the functionalised oxide samples.

References

[1] Yao X, Song YL, Jiang L (2011) Applications of Bio-Inspired Special Wettable Surfaces, Adv Mater 23:719-734.

[2] Spori DM, Drobek T, Zurcher S, Ochsner M, Sprecher C, Muehlebach A, Spencer ND (2008) Beyond the lotus effect: Roughness, influences on wetting over a wide surface-energy range, Langmuir 24:5411-5417.

[3] Spori DM, Venkataraman NV, Tosatti SGP, Durmaz F, Spencer ND, Zurcher S (2007) Influence of alkyl chain length on phosphate self-assembled monolayers, Langmuir 23:8053-8060.

[4] Meroni D, Ardizzone S, Cappelletti G, Ceotto M, Ratti M, Annunziata R, Benaglia M, Raimondi L (2011) Interplay between Chemistry and Texture in Hydrophobic TiO_2 Hybrids, J Phys Chem C 115:18649-18658.

[5] Quere D (2008) Wetting and roughness, Annu Rev Mater Res 38:71-99.

[6] Sagiv J (1980) Organized monolayers by adsorption. 1. Formation and Structure of Oleophobic Mixed Monolayers on Solid Surfaces, J Am Chem Soc 102:92-98.

[7] Meroni D, Ardizzone S, Schubert US, Hoeppener S (2012) Probe-Based Electro-Oxidative Lithography of OTS SAMs Deposited onto Transparent ITO Substrates, Adv Funct Mater 22:4376-4382.

[8] Hozumi A, Ushiyama K, Sugimura H, Takai O (1999) Fluoroalkylsilane monolayers formed by chemical vapor surface modification on hydroxylated oxide surfaces, Langmuir 15:7600-7604.

[9] Zhang F, Sautter K, Larsen AM, Findley DA, Davis RC, Samha H, Linford MR (2010) Chemical Vapor Deposition of Three Aminosilancs on Silicon Dioxide: Surface Characterization, Stability, Effects of Silane Concentration, and Cyanine Dye Adsorption, Langmuir 26:14648-14654.

[10] Zhu MJ, Lerum MZ, Chen W (2012) How To Prepare Reproducible, Homogeneous, and Hydrolytically Stable Aminosilane-Derived Layers on Silica, Langmuir 28:416-423.

[11] Onclin S, Ravoo BJ, Reinhoudt DN (2005) Engineering silicon oxide surfaces using self-assembled monolayers, Angew Chem Int Edit 44:6282-6304.

[12] Koga T, Morita M, Ishida H, Yakabe H, Sasaki S, Sakata O, Otsuka H, Takahara A (2005) Dependence of the molecular aggregation state of octadecylsiloxane monolayers on preparation methods, Langmuir 21:905-910.

[13] Bravo J, Zhai L, Wu ZZ, Cohen RE, Rubner MF (2007) Transparent superhydrophobic films based on silica nanoparticles, Langmuir 23:7293-7298.

[14] Maino G, Meroni D, Pifferi V, Falciola L, Soliveri G, Cappelletti G, Ardizzone S Electrochemically assisted deposition of transparent, mechanically robust TiO_2 films for advanced applications, Journal of Nanoparticle Research, in press.

[15] Meroni D, Ardizzone S, Cappelletti G, Oliva C, Ceotto M, Poelman D, Poelman H (2011) Photocatalytic removal of ethanol and acetaldehyde by N-promoted TiO_2 films: The role of the different nitrogen sources, Catal Today 161:169-174.

[16] Paz YR (2011) Self-assembled monolayers and titanium dioxide: From surface patterning to potential applications, Beilstein J Nanotech 2:845-861.

[17] JCPDS-ICDD card n. 21-1272 (2002) International Centre for Diffraction Data, Newtown Square, PA.

[18] Cappelletti G, Ardizzone S, Meroni D, Soliveri G, Ceotto M, Biaggi C, Benaglia M, Raimondi L (2013) Wettability of bare and fluorinated silanes: A combined approach based on surface free energy evaluations and dipole moment calculations, J Colloid Interf Sci 389:284-291.

[19] Milanesi F, Cappelletti G, Annunziata R, Bianchi CL, Meroni D, Ardizzone S (2010) Siloxane-TiO2 Hybrid Nanocomposites. The Structure of the Hydrophobic Layer, J Phys Chem C 114:8287-8293.

[20] Soliveri G, Annunziata R, Ardizzone S, Cappelletti G, Meroni D (2012) Multiscale Rough Titania Films with Patterned Hydrophobic/Oleophobic Features, J Phys Chem C 116:26405-26413.

[21] Puglisi A, Annunziata R, Benaglia M, Cozzi F, Gervasini A, Bertacche V, Sala MC (2009) Hybrid Inorganic-Organic Materials Carrying Tertiary Amine and Thiourea Residues Tethered on Mesoporous Silica Nanoparticles: Synthesis, Characterization, and Co-Operative Catalysis, Adv Synth Catal 351:219-229.

[22] Legrand A (1998) The Surface Properties of Silicas. John Wiley, New York

[23] Morterra C (1988) An Infrared Spectroscopic Study of Anatase Properties .6. Surface Hydration and Strong Lewis Acidity of Pure and Sulfate-Doped Preparations, J Chem Soc Farad T 1 84:1617-1637.

[24] Bellamy L (1968) Advances in Infra-red Group Frequencies. Methuen, London

[25] Vallant T, Kattner J, Brunner H, Mayer U, Hoffmann H (1999) Investigation of the formation and structure of self-assembled alkylsiloxane monolayers on silicon using in situ attenuated total reflection infrared spectroscopy, Langmuir 15:5339-5346.

[26] Chang HY, Thangamuthu R, Lin CW (2004) Structure-property relationships in PEG/SiO_2 based proton conducting hybrid membranes - A Si-29 CP/MAS solid-state NMR study, J Membrane Sci 228:217-226.

[27] Brodard-Severac F, Guerrero G, Maquet J, Florian P, Gervais C, Mutin PH (2008) High-Field O-17 MAS NMR Investigation of Phosphonic Acid Monolayers on Titania, Chem Mater 20:5191-5196.

[28] Huh S, Chen HT, Wiench JW, Pruski M, Lin VSY (2005) Cooperative catalysis by general acid and base bifunctionalized mesoporous silica nanospheres, Angew Chem Int Edit 44:1826-1830.

[29] Kovacek D, Maksic ZB, Elbel S, Kudnig J (1994) Semiempirical Calculation of Si-29 Nmr Chemical-Shifts and Si-29-C-13 Spin-Spin Coupling-Constants in Some Substituted Bridgehead Polycycloalkanes, J Mol Struc-Theochem 110:247-254.

[30] Huh S, Wiench JW, Yoo JC, Pruski M, Lin VSY (2003) Organic functionalization and morphology control of mesoporous silicas via a co-condensation synthesis method, Chem Mater 15:4247-4256.

[31] Kujawa J, Kujawski W, Koter S, Rozicka A, Cerneaux S, Persin M, Larbot A (2013) Efficiency of grafting of Al_2O_3, TiO_2 and ZrO_2 powders by perfluoroalkylsilanes, Colloid Surface A 420:64-73.

[32] Moriguchi T, Murase K, Sugimura H (2008) Ruthenium-amine complexation for constructing self-assembled molecular films, Colloid Surface A 321:94-98.

[33] Sugimura H, Moriguchi T, Kanda M, Sonobayashi Y, Nishimura HM, Ichii T, Murase K, Kazama S (2011) Molecular packing density of a self-assembled monolayer formed from N-(2-aminoethyl)-3-aminopropyltriethoxysilane by a vapor phase process, Chem Commun 47:8841-8843.

[34] Wenzel R (1936) Resistance of Solid Surfaces to Wetting by Water, Ind Eng Chem 28:988–994.

[35] Cassie AB, S. (1944) Wettability of porous surfaces, Trans Farad Soc 40:546–551.

[36] Nosonovsky M, Bhushan B (2009) Superhydrophobic surfaces and emerging applications: Non-adhesion, energy, green engineering, Curr Opin Colloid In 14:270-280.

[37] Kim WJ, Kim S, Lee BS, Kim A, Ah CS, Huh C, Sung GY, Yun WS (2009) Enhanced Protein Immobilization Efficiency on a TiO_2 Surface Modified with a Hydroxyl Functional Group, Langmuir 25:11692-11697.

Table 1. Relative percentages of the different T^X structures and width at half height ($\Delta\nu_{1/2}$) of each resonance obtained by the fitting analysis of the ^{29}Si NMR spectra of the T-216 samples.

	T-216 CVD			T-216 WI		
	δ ppm	**%**	**$\Delta\nu_{1/2}$ Hz**	**δ ppm**	**%**	**$\Delta\nu_{1/2}$ Hz**
T^1	-51	47	982	-51	39	949
T^2_{Si} / T^2_{Ti}	-59	39	656	-59	48	699
T^3	-68	14	692	-68	13	610

Table 2. Water advancing contact angles (θ_a) and contact angle hystereses ($\Delta\theta$) of the oxide films functionalised by CVD and WI.

Sample	CVD		WI	
	θ_a	$\Delta\theta$	θ_a	$\Delta\theta$
S-6	147 ± 2	< 5	118 ± 4	40
T-3	123 ± 4	34	101 ± 6	44
T-216	> 150	< 5	> 150	< 5

Figure captions

Figure 1. Particle size distribution curves (intensity vs. particle diameter) of the three oxide powders determined by DLS analysis. Inset: Particle size distribution (average size and relative amount (%amt) of the different size populations) obtained by DLS (2^{nd} and 3^{rd} column), SEM analyses (4^{th} column), and specific surface area by BET analysis (5^{th} column) of the different oxides.

Figure 2. SEM imagines of the oxide particles: a) T-3, b) S-6, c) T-216.

Figure 3. FTIR spectra, in the 3900-1350 spectral range, of S-6 (Section A) and T-216 (Section B) pristine (dashed line, spectrum a) and either functionalised via WI (thin solid line, spectrum b) or CVD (thick solid line, spectrum c). Inset: differential FTIR spectra: the b) – a) trace refers to a differential absorbance spectrum obtained by subtracting curve a) (pristine samples) from curve b) (WI functionalised samples); the c) – a) trace refers to a differential absorbance spectrum obtained by subtracting curve a) (pristine samples) from curve c) (CVD functionalised samples).

Figure 4.The ^{13}C MAS NMR spectra of SiO_2 (a and b) and TiO_2 (c and d) hybrids obtained by WI and CVD methods, respectively.

Figure 5. ^{29}Si CP/MAS NMR spectra of the different siloxane-oxide hybrids: S-6 from WI (a) and CVD (b), T-216 from WI (c) and CVD (d).

Figure 6. Water static contact angle of S-6 functionalised by CVD (a) and WI (b). Sketches of contact angle on rough surfaces according to Cassie-Baxter (c) and Wenzel (d) descriptions.

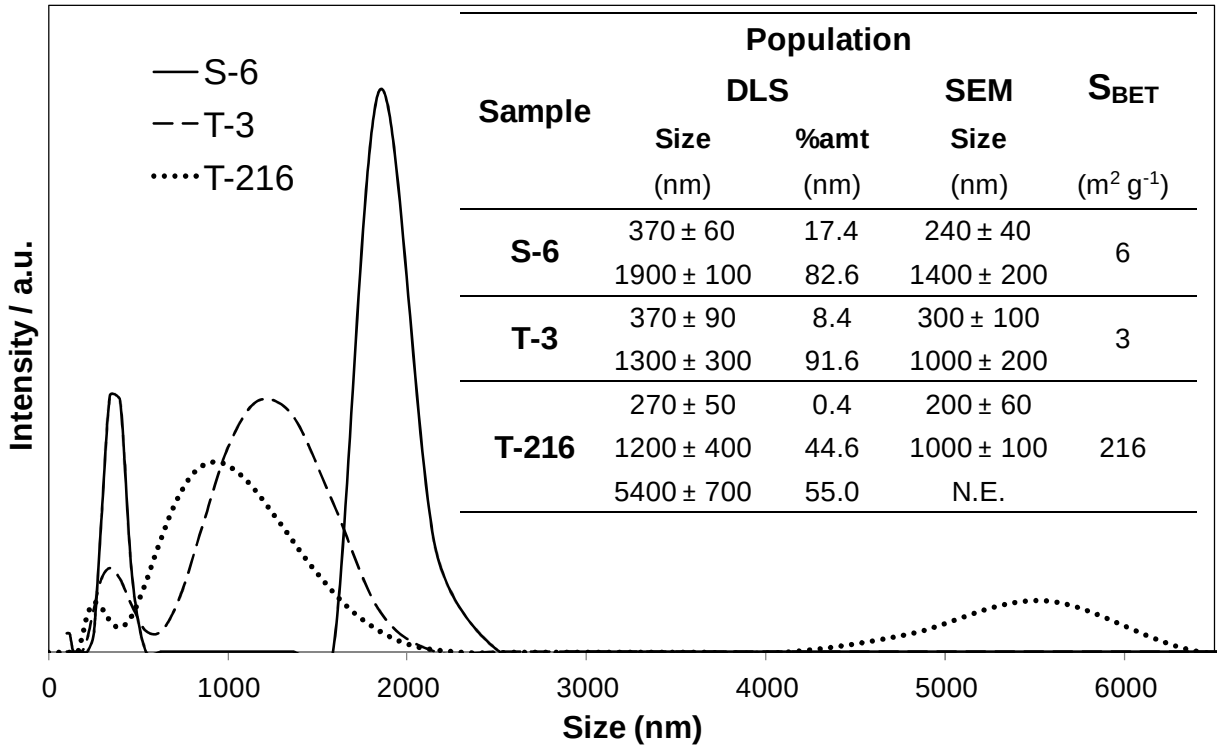

Sample	Population DLS Size (nm)	DLS %amt (nm)	SEM Size (nm)	S_{BET} ($m^2\ g^{-1}$)
S-6	370 ± 60	17.4	240 ± 40	6
	1900 ± 100	82.6	1400 ± 200	
T-3	370 ± 90	8.4	300 ± 100	3
	1300 ± 300	91.6	1000 ± 200	
T-216	270 ± 50	0.4	200 ± 60	216
	1200 ± 400	44.6	1000 ± 100	
	5400 ± 700	55.0	N.E.	

FIGURE 1

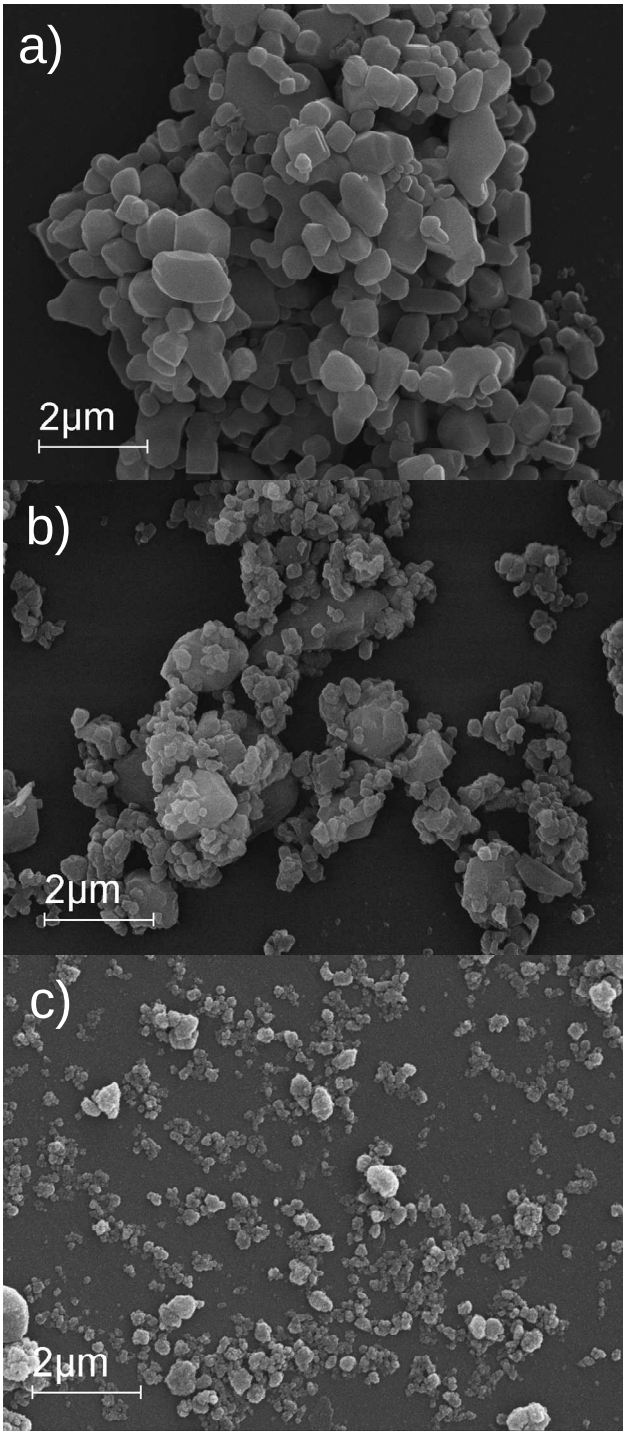

FIGURE 2

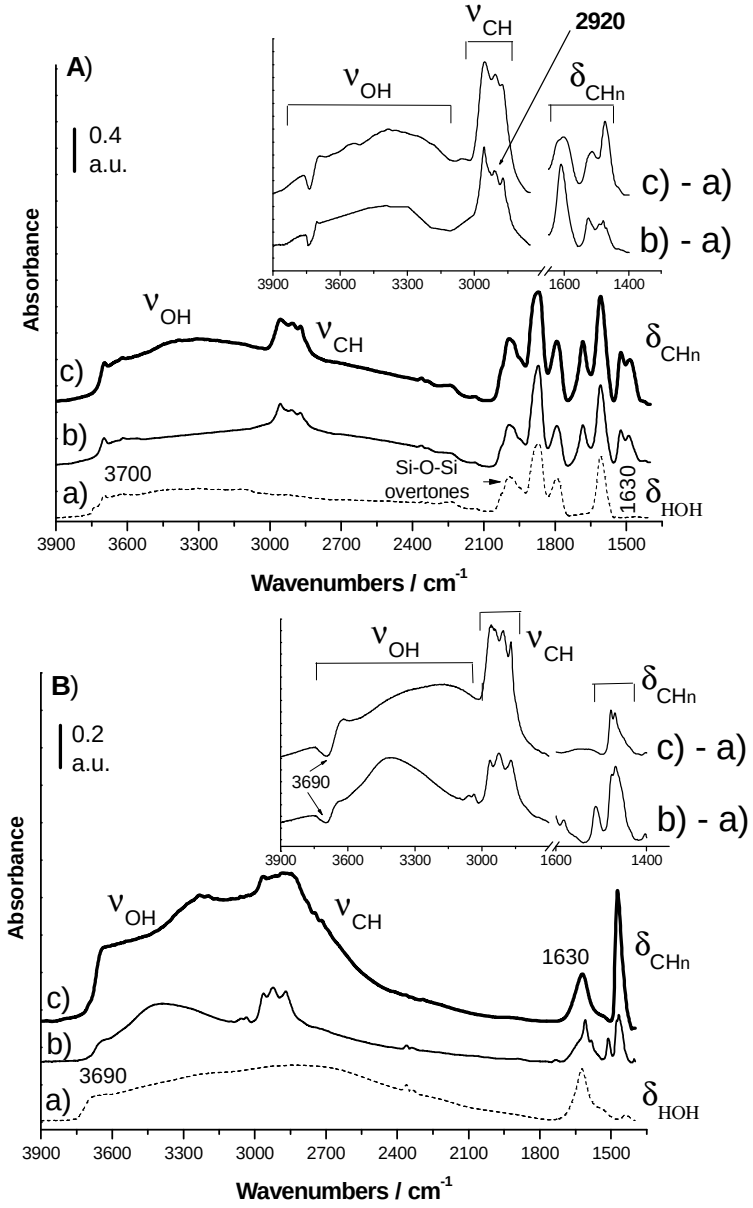
A)
0.4
a.u.
Absorbance
ν_{OH}
ν_{CH}
2920
δ_{CHn}
c) - a)
b) - a)
3900 3600 3300 3000 1600 1400
ν_{OH}
ν_{CH}
δ_{CHn}
c)
b)
3700
Si-O-Si
overtones
1630
δ_{HOH}
a)
3900 3600 3300 3000 2700 2400 2100 1800 1500
Wavenumbers / cm^{-1}
B)
0.2
a.u.
Absorbance
ν_{OH}
ν_{CH}
δ_{CHn}
3690
c) - a)
b) - a)
3900 3600 3300 3000 1600 1400
ν_{OH}
ν_{CH}
1630
δ_{CHn}
c)
b)
3690
a)
δ_{HOH}
3900 3600 3300 3000 2700 2400 2100 1800 1500
Wavenumbers / cm^{-1}

FIGURE 3

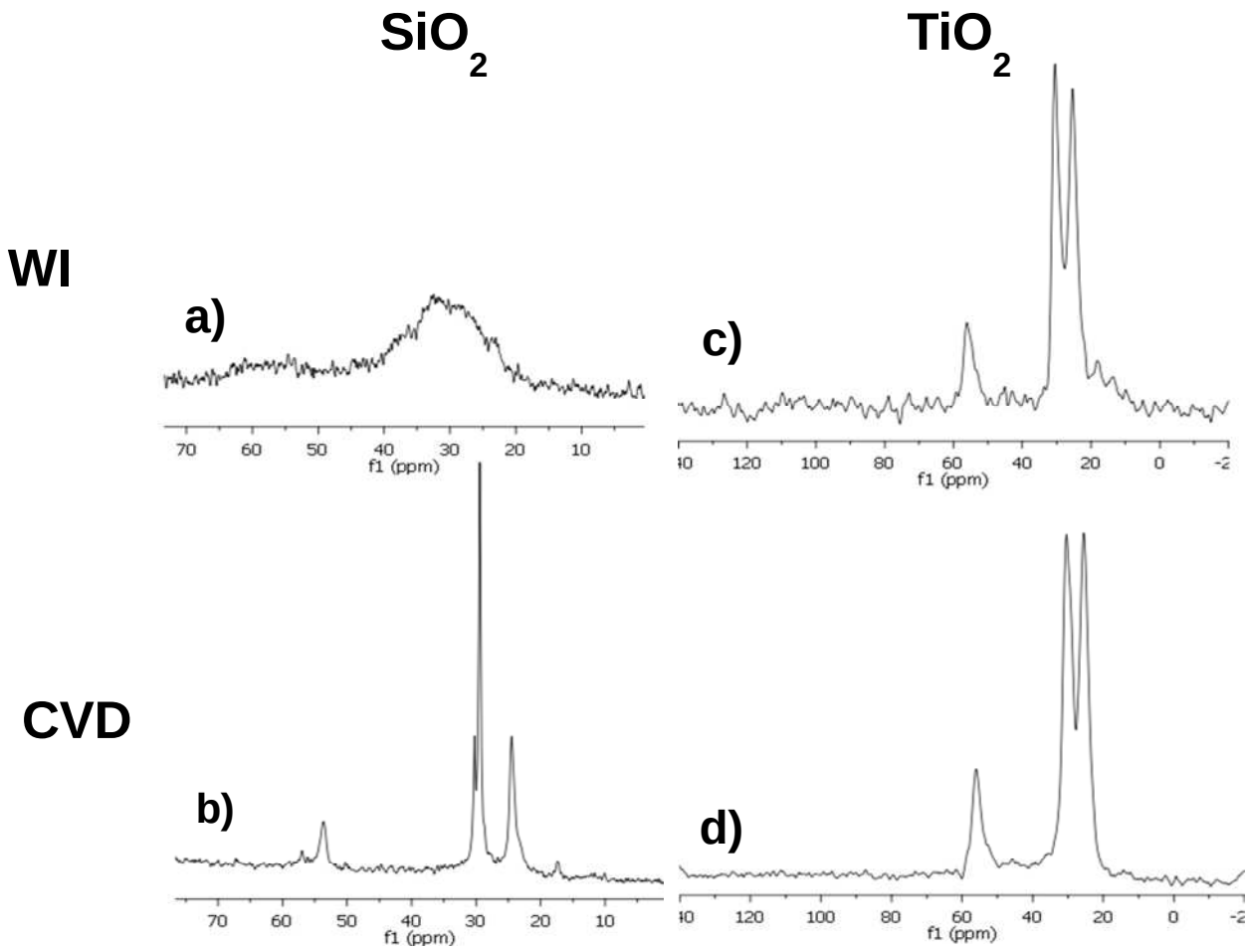

FIGURE 4

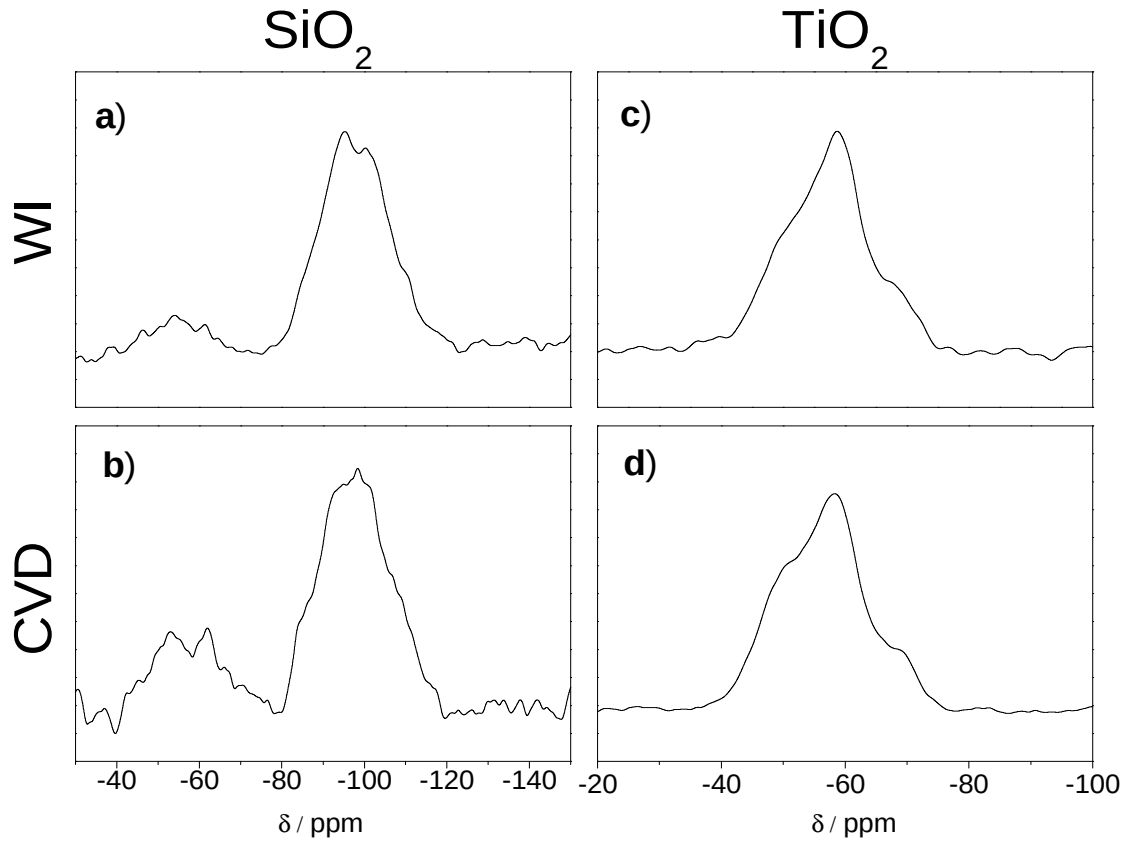
SiO2
TiO2
WI
CVD
a)
b)
c)
d)
-40
-60
-80
-100
-120
-140
-20
-40
-60
-80
-100
δ / ppm
δ / ppm

FIGURE 5

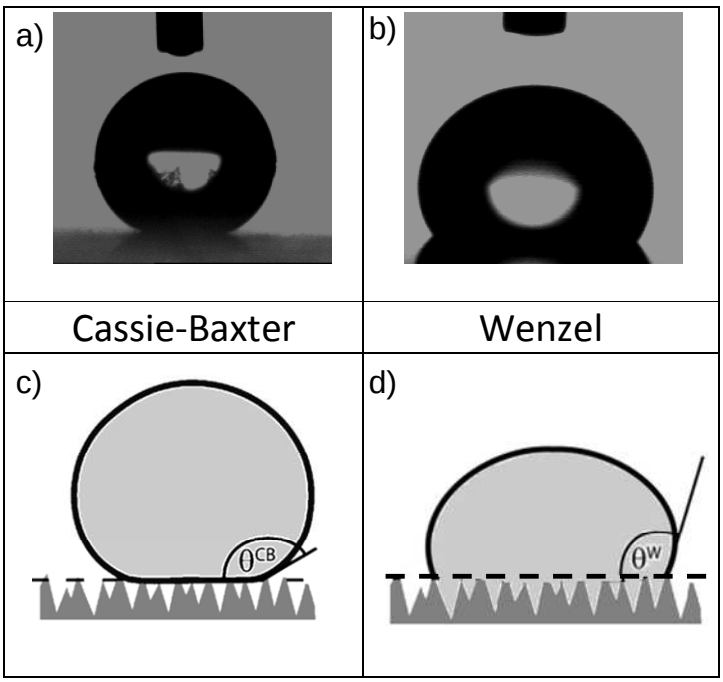

FIGURE 6